Identification and Quantitation of Dibenzo[*a*,*l*]pyrene−DNA Adducts Formed by Rat Liver Microsomes *in Vitro*: Preponderance of Depurinating Adducts†

K.-M. Li,‡ R. Todorovic,‡ E. G. Rogan,‡ E. L. Cavalieri,*,‡ F. Ariese,§,|| M. Suh,§,|| R. Jankowiak,|| and G. J. Small§,||

Eppley Institute for Research in Cancer, University of Nebraska Medical Center, Omaha, Nebraska 68198-6805, and Department of Chemistry and Ames Laboratory, USDOE, Iowa State University, Ames, Iowa 50011

Received November 22, 1994; Revised Manuscript Received April 24, 1995⊗

ABSTRACT: Dibenzo[*a*,*l*]pyrene (DB[*a*,*l*]P) is the most potent carcinogen known among aromatic hydrocarbons. DB[*a*,*l*]P-11,12-dihydrodiol, precursor to the bay-region diol epoxide, is slightly less carcinogenic than the parent compound. DB[*a*,*l*]P and its 11,12-dihydrodiol were covalently bound to DNA by cytochrome P-450 in 3-methylcholanthrene-induced rat liver microsomes, and DB[*a*,*l*]P was also bound to DNA by horseradish peroxidase. The "stable" (remaining intact in DNA under normal conditions of purification) and "depurinating" (released from DNA by cleavage of the glycosidic link between the purine base and deoxyribose) adducts were identified and quantified. Stable adducts were analyzed by the ^{32}P-postlabeling technique. Depurinating adducts were identified by comparison of their retention times with those of standard adducts on HPLC in two solvent systems. Confirmation of their identity was obtained by means of fluorescence line-narrowing spectroscopy. When DB[*a*,*l*]P was activated by horseradish peroxidase, the depurinating adducts 3-(DB[*a*,*l*]P-10-yl)adenine (DB[*a*,*l*]P-10-N3Ade, 33%), 7-(DB[*a*,*l*]P-10-yl)adenine (DB[*a*,*l*]P-10-N7Ade, 27%), and 7-DB[*a*,*l*]P-10-yl)guanine (DB[*a*,*l*]P-10-N7Gua, 5%) were formed. Unidentified stable adducts comprised the remaining 35% of the detected adducts. When DB[*a*,*l*]P was activated by microsomes, the one-electron oxidation depurinating adducts DB[*a*,*l*]P-10-N3Ade (28%), DB[*a*,*l*]P-10-N7Ade (14%), DB[*a*,*l*]P-10-N7Gua (2%), and DB[*a*,*l*]P-10-C8Gua (6%), as well as the diol epoxide depurinating adducts (±)-*syn*-DB[*a*,*l*]P-diol epoxide (DE)-14-N7Ade (31%) and (±)-*anti*-DB[*a*,*l*]PDE-14-N7Gua (3%), were formed. Stable adducts predominantly formed via the DB[*a*,*l*]PDE pathway represented 16% of the adducts detected. When DB[*a*,*l*]P-11,12-dihydrodiol was activated by microsomes, the same two depurinating adducts arising from DB[*a*,*l*]PDE were found, but they constituted only 19% of the adducts because the amount of stable adducts was much higher than with DB[*a*,*l*]P. Analysis of stable DNA adducts by the ^{32}P-postlabeling method indicates that the profiles formed from DB[*a*,*l*]P and its 11,12-dihydrodiol were qualitatively similar. These results demonstrate that the major depurinating adducts formed by both DB[*a*,*l*]P and its 11,12-dihydrodiol are at the N-3 and N-7 of adenine, resulting in apurinic sites in the DNA.

Dibenzo[*a*,*l*]pyrene (DB[*a*,*l*]P)[1] (Figure 1) has been shown to be the most potent carcinogen among PAH (Cavalieri et al., 1989, 1991; Higginbotham et al., 1993; LaVoie et al., 1993). The carcinogenicity of DB[*a*,*l*]P in rat mammary gland and mouse skin was found to be significantly stronger than that of DMBA, previously considered to be the most potent PAH, and BP, previously considered to be the most potent environmental PAH (Cavalieri et al., 1991; Higginbotham et al., 1993). DB[*a*,*l*]P has been tentatively identified in a biologically-active fraction of cigarette smoke condensate (Snook et al., 1977). It is thought to be a component of other pollutants (IARC, 1983). Definitive identification in the environment has been obtained in the particulates formed by combustion of smoky coal (Mumford et al., 1987, 1995).

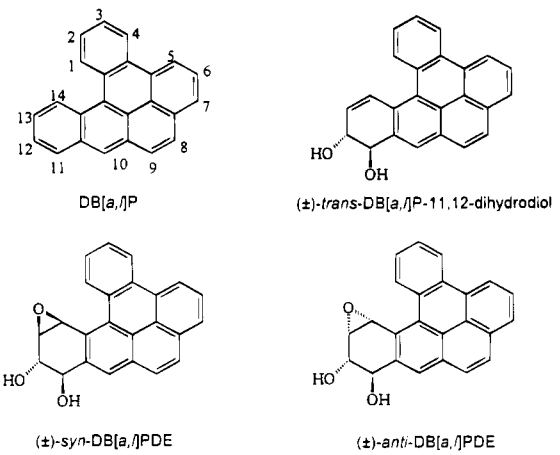

FIGURE 1: Structures of DB[*a*,*l*]P and some of its metabolites.

† Supported by U.S. Public Health Service Grants R01-CA49917 and P01-CA49210 from the National Cancer Institute. Core support at the Eppley Institute was provided by the National Cancer Institute (P30-CA36727).

* To whom correspondence should be addressed.
‡ University of Nebraska Medical Center.
§ Department of Chemistry, Iowa State University.
|| Ames Laboratory, Iowa State University.

⊗ Abstract published in *Advance ACS Abstracts,* June 1, 1995.

[1] Abbreviations: BP, benzo[*a*]pyrene; BPDE, (±)-(7*r*)-*trans*-8-dihydroxy-*trans*-9,10-epoxy-7,8,9,10-tetrahydrobenzo[*a*]pyrene; DB-[*a*,*l*]P, dibenzo[*a*,*l*]pyrene; DB[*a*,*l*]PDE, dibenzo[*a*,*l*]pyrenediol epoxide; DB[*a*,*l*]P-10-C8Gua, 8-(dibenzo[*a*,*l*]pyren-10-yl)guanine; DB[*a*,*l*]P-10-N3Ade, 3-(dibenzo[*a*,*l*]pyren-10-yl)adenine; DB[*a*,*l*]P-10-N7Ade, 7-(dibenzo[*a*,*l*]pyren-10-yl)adenine; DB[*a*,*l*]P-10-N7Gua, 7-(dibenzo-[*a*,*l*]pyren-10-yl)guanine; DMBA, 7,12-dimethylbenz[*a*]anthracene; FLNS, fluorescence line-narrowing spectroscopy; HPLC, high-pressure liquid chromatography; HRP, horseradish peroxidase; MC, 3-methylcholanthrene; PAH, polycyclic aromatic hydrocarbon(s); (±)-*syn*-DB-[*a*,*l*]PDE-14-N7Ade, (±)-*syn*-14-(adenin-7-yl)-11,12,13-trihydroxy-11,12,13,14-tetrahydrodibenzo[*a*,*l*]pyrene; (±)-*anti*-DB[*a*,*l*]PDE-14-N7Gua, (±)-*anti*-14-(guanin-7-yl)-11,12,13-trihydroxy-11,12,13,14-tetrahydrodibenzo[*a*,*l*]pyrene.

0006-2960/95/0434-8043$09.00/0

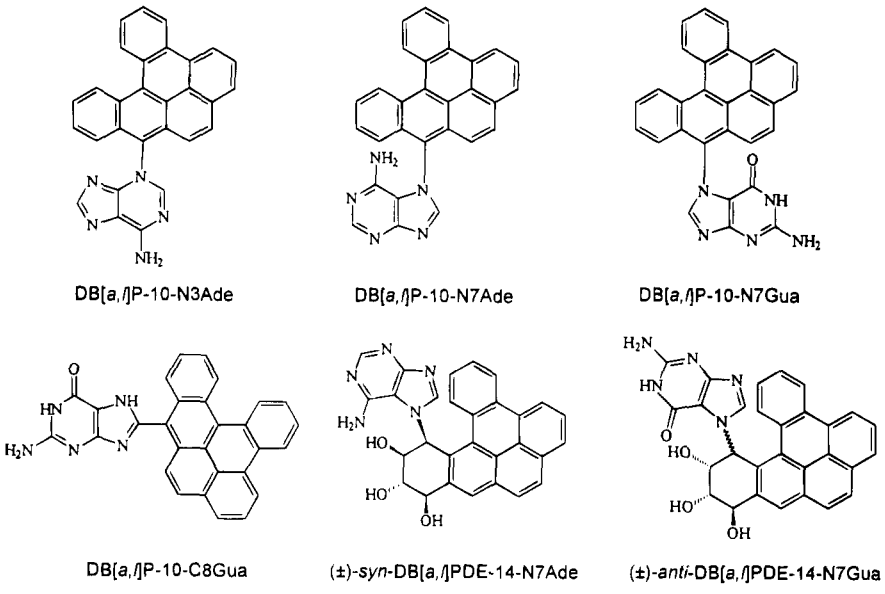

FIGURE 2: Structures of DB[*a,l*]P−DNA adducts identified *in vitro*.

Like other PAH, DB[*a,l*]P is activated by two main mechanisms: one-electron oxidation to yield reactive intermediate radical cations (Cavalieri & Rogan, 1985, 1992) and monooxygenation to yield bay-region diol epoxides (Conney, 1982; Sims & Grover, 1981). The active intermediates formed by the two mechanisms, radical cations and bay-region diol epoxides, can bind to DNA, presumably initiating the process of tumor formation. DNA adducts can be divided into two categories based on their retention in DNA. "Stable" adducts remain intact in DNA under normal conditions of isolation. In contrast, "depurinating" adducts are released from DNA by depurination, the process in which the bond between the purine base and deoxyribose is hydrolyzed. For example, adducts containing BP or DMBA bound to the N-7 of adenine or guanine are depurinating adducts because binding of BP or DMBA at the N-7 causes rapid hydrolysis of the glycosidic bond (Cavalieri et al., 1990; Devanesan et al., 1992, 1993; RamaKrishna et al., 1992a,b; Rogan et al., 1993). The adduct containing BP bound at the C-8 of guanine is also a depurinating adduct, although the glycosidic link is hydrolyzed more slowly (Cavalieri et al., 1990; Devanesan et al., 1992; RamaKrishna et al., 1992b; Rogan et al., 1993). In contrast, the adduct containing BP-diol epoxide bound at the 2-amino group of dG is stable, and this adduct is found in intact DNA (Bodell et al., 1989; Devanesan et al., 1992; Jeffrey et al., 1976; Koreeda et al., 1978; Rogan et al., 1993).

When BP is activated by MC-induced rat liver microsomes or mouse skin *in vivo*, 75−80% of the adducts detected are formed by one-electron oxidation of BP and are lost from DNA by depurination (Devanesan et al., 1992; Rogan et al., 1993). The stable adduct formed by BP-diol epoxide at the 2-amino group of dG comprises 15−22% of the adducts detected. With DMBA, 99% of the adducts detected in mouse skin or *in vitro* are depurinating adducts formed by one-electron oxidation, with the stable adducts formed from DMBA-diol epoxide comprising less than 0.2% of the total adducts (RamaKrishna et al., 1992a; Devanesan et al., 1993).

By modeling our study of DB[*a,l*]P−DNA adducts on our successful studies of BP− and DMBA−DNA adducts, reference adducts of DB[*a,l*]P have been synthesized. Electrochemical oxidation of DB[*a,l*]P in the presence of dA or dG produces five adducts formed from DB[*a,l*]P radical cation (RamaKrishna et al., 1993). Reaction of the (±)-*syn*- or (±)-*anti*-DB[*a,l*]PDE (Figure 1) with dA or dG yields 13 adducts (Li et al., 1994, 1995a). These adducts are used as reference standards in the identification of depurinating and stable adducts of DB[*a,l*]P formed *in vitro*. In this paper qualitative and quantitative analyses of the depurinating adducts obtained by microsomal activation of DB[*a,l*]P or DB[*a,l*]P-11,12-dihydrodiol (Figure 1) and HRP-catalyzed activation of DB[*a,l*]P are reported. With activation by cytochrome P-450, adducts are obtained by both mechanisms, whereas with HRP, activation occurs only by one-electron oxidation (Rogan et al., 1979, 1988).

EXPERIMENTAL PROCEDURES

Chemicals. DB[*a,l*]P (mp 161−162 °C) was obtained from the National Cancer Institute Chemical Carcinogen Repository, Bethesda, MD. It was used as received, after analysis by reverse-phase HPLC on a Waters Millennium 2010 chromatography system with a 996 photodiode array detector and a YMC ODS-AQ S-5 120 Å (6 × 250 mm) column with a CH_3CN/H_2O gradient that showed its purity was >99%. [^{3}H]DB[*a,l*]P was prepared by Chemsyn Science Laboratories, Lenexa, KS, purified by HPLC to >99% purity, and used at a specific activity of 240 Ci/mol. [^{3}H]-DB[*a,l*]P-11,12-dihydrodiol was synthesized enzymatically (Devanesan et al., 1990) and purified by HPLC (Cavalieri et al., 1991).

The depurinating adduct standards DB[*a,l*]P-10-N7Ade, DB[*a,l*]P-10-N7Gua, and DB[*a,l*]P-10-C8Gua (Figure 2) were obtained by electrochemical oxidation in the presence of dA or dG (RamaKrishna et al., 1993). DB[*a,l*]P-10-N3Ade was obtained by electrochemical oxidation in the presence of adenine (Li et al., 1995b). (±)-*syn*-DB[*a,l*]PDE-14-N7Ade, (±)-*anti*-DB[*a,l*]PDE-14-N7Gua, and (±)-*syn*-DB[*a,l*]PDE-14-N7Gua were synthesized by reacting the diol epoxides with dA or dG (Li et al., 1994, 1995a).

For reactions with single-stranded DNA, calf thymus DNA (Pharmacia, Piscataway, NJ) was denatured by heating in a boiling water bath for 5 min followed by quick cooling in ice−water.

Binding of [^{3}H]DB[a,l]P and [^{3}H]DB[a,l]P-11,12-dihydrodiol to DNA. As previously described (Bodell et al., 1989), [^{3}H]DB[*a,l*]P (80 μM) and [^{3}H]DB[*a,l*]P-11,12-dihydrodiol (80 μM) were bound to native or denatured DNA in reactions catalyzed by MC-induced rat liver microsomes. [^{3}H]DB[*a,l*]P (80 μM) was also bound to native DNA in a HRP-catalyzed reaction. The reactions with [^{3}H]DB[*a,l*]P were 15 mL in volume, whereas those with [^{3}H]DB[*a,l*]P-11,12-dihydrodiol were 10 mL. They were all incubated at 37 °C for 30 min. At the end of the reaction, a 1-mL aliquot of the mixture was used to determine the level of DB[*a,l*]P and DB[*a,l*]P-11,12-dihydrodiol binding to DNA and to analyze stable adducts by the ^{32}P-postlabeling method (Bodell et al., 1989). The DNA from the remaining 14 (or 9)-mL mixture was precipitated with 2 volumes of absolute ethanol, and the supernatant was used to identify and quantify the depurinating adducts by HPLC and FLNS.

Detection of DB[a,l]P- and DB[a,l]P-11,12-dihydrodiol−DNA Depurinating Adducts by HPLC. The supernatant from the incubation was evaporated under vacuum, and the residue was extracted with DMSO/CH_3OH (1:1). The sample solution was first analyzed for the six depurinating adducts (Figure 2) on a CH_3CN/H_2O gradient (5 min at 80% H_2O/20% CH_3CN, a 75-min linear gradient to 100% CH_3CN, and 20 min at 100% CH_3CN at a flow rate of 1.0 mL/min). Fractions were collected at the elution time of each synthetic standard adduct (Figure 3A). Each fraction was evaporated under vacuum, and the residue was redissolved in DMSO/CH_3OH (1:1). These solutions were then analyzed on a CH_3OH/H_2O gradient (5 min at 70% H_2O/30% CH_3OH, a 70-min linear gradient to 100% CH_3OH, and 20 min at 100% CH_3OH at a flow rate of 1.0 mL/min) with a Waters 996 photodiode array detector, a Jasco FP-920 fluorescence detector, and a radiation flow monitor connected in series, as shown for DB[*a,l*]P-10-N3Ade in Figure 3B. Radioactive peaks with retention times matching those of the standard adducts in the two different HPLC gradients were tentatively identified as adducts. Confirmation of the structure of biologically-formed adducts was obtained by FLNS. For each putative adduct peak, at least three fractions were collected and analyzed by FLNS to provide evidence on the purity of the peak. For example, in Figure 3B the fraction adjacent to the left side of the DB[*a,l*]P-10-N3Ade peak was determined by FLNS to be unrelated to the adduct.

Analysis of Depurinating Adducts by FLNS. Collected HPLC fractions were evaporated to dryness, stored at −20 °C, and dissolved prior to spectroscopic measurements by adding a glass-forming solvent mixture to each sample vial followed by sonication for 10 min at 35 °C (water/glycerol/ethanol, 40:40:20, for the one-electron oxidation adducts; water/glycerol, 50:50, for the monooxygenation adducts). Each sample solution (20 μL) was transferred to a 1.7-mm i.d. quartz tube and sealed with a rubber septum.

A detailed description of the apparatus used for FLN spectroscopy is given elsewhere (Jankowiak & Small, 1991). Briefly, the excitation source was a λ-Physik FL-2002 dye laser, pumped by a λ-Physik EMG 102 MSC XeCl excimer laser. Stilbene-3 in ethanol was used as the laser dye for the one-electron oxidation adducts (excitation region 414−419 nm); QUI in dioxane was used for the monooxygenation adducts (374−382 nm). Samples were cooled to 4.2 K in a helium bath cryostat. Fluorescence was dispersed by a 1-m focal length MePherson 2016 monochromator with a 2400 grooves/mm grating, providing an 8-nm spectral window (resolution 0.08 nm) for the Princeton Instruments IRY 1024/G/B intensified blue-enhanced photodiode array detector. For gated detection the output of a reference photodiode was used to trigger an FG-100 high-voltage gate pulse generator; the detector delay time was set to 45 ns; the gate width was 200 ns.

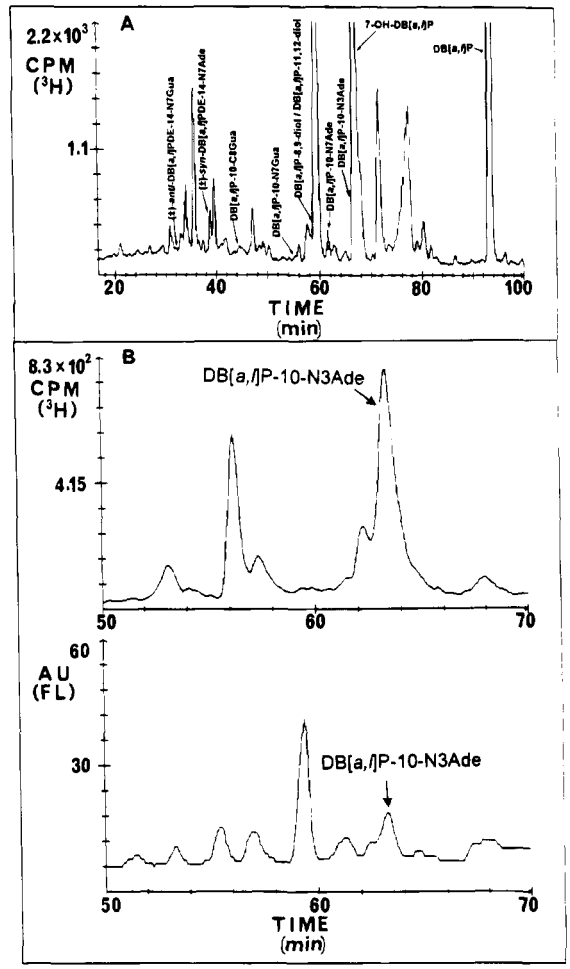

FIGURE 3: HPLC separation of depurinating adducts. (A) First separation of adduct mixture on the CH_3CN/H_2O gradient, monitored by radioactivity, and (B) purification of the DB[*a,l*]P-10-N3Ade adduct collected in panel A with the CH_3OH/H_2O gradient, monitored by radioactivity (top) and fluorescence (bottom).

Calculation of Adduct Levels. The amount of stable adducts was calculated by the ^{32}P-postlabeling method as previously described (Bodell et al., 1989). For quantitation of the depurinating adducts, each of the peaks eluting at the same time as an authentic adduct in HPLC using the CH_3CN/H_2O gradient was collected and the radioactivity counted. These peaks were then reinjected individually in the CH_3OH/H_2O gradient and the percentage of the injected radioactivity eluting at the same time as the authentic adduct was measured and calculated using the radiation flow monitor. The total amount of each of the adducts was calculated from the specific activity of DB[*a,l*]P and normalized to the amount of DNA used in the reaction.

RESULTS

Identification of DNA Adducts. To characterize the DB[*a,l*]P−DNA adducts formed by cytochrome P-450 in MC-induced rat liver microsomes, the adducts were compared

to those formed in two systems that yield DNA adducts by only one mechanism. Formation of adducts of DB[*a*,*l*]P by one-electron oxidation was compared to the DB[*a*,*l*]P adducts obtained by activation with HRP. Cytochrome P-450 activation of DB[*a*,*l*]P-11,12-dihydrodiol provided adducts derived from the bay-region diol epoxide. The stable adducts were quantified and identified by the ^{32}P-postlabeling technique (Bodell et al., 1989). The depurinating adducts were identified by comparison with authentic adduct standards obtained by electrochemical oxidation of DB[*a*,*l*]P in the presence of dA, dG, or Ade (RamaKrishna et al., 1993; Li et al., 1995b) or by reaction of DB[*a*,*l*]PDE with dA or dG (Li et al., 1994, 1995a). Preliminary identification of these adducts was made by coelution with authentic adducts on HPLC in the two different solvent systems (Figure 3). Definite proof of the structures was obtained by FLNS analysis.

Rat liver microsomes in the presence of DNA produced four depurinating adducts formed by the radical cation pathway, DB[*a*,*l*]P-10-N3Ade, DB[*a*,*l*]P-10-N7Ade, DB-[*a*,*l*]P-10-N7Gua, and DB[*a*,*l*]P-10-C8Gua, and two by the diol epoxide pathway, (±)-*syn*-DB[*a*,*l*]PDE-14-N7Ade and (±)-*anti*-DB[*a*,*l*]PDE-14-N7Gua (Table 1, Figure 2). Only DB[*a*,*l*]P-10-N3Ade, DB[*a*,*l*]P-10-N7Ade, and DB[*a*,*l*]P-10-N7Gua were formed when DB[*a*,*l*]P was activated by HRP (Table 1). The recent synthesis of DB[*a*,*l*]P-10-N3Ade by electrochemical oxidation of DB[*a*,*l*]P in the presence of Ade (Li et al., 1995b) enabled us to demonstrate that this adduct is formed enzymatically. The two depurinating diol epoxide adducts obtained from DB[*a*,*l*]P were also formed by microsomal activation of the proximate metabolite DB[*a*,*l*]P-11,12-dihydrodiol (Table 1). The (±)-*anti*-DB[*a*,*l*]PDE-14-N7Ade adduct may have been formed but could not be detected because the standard adduct was not available. With microsomal activation, the stable adducts of DB[*a*,*l*]P appeared to arise almost entirely from the diol epoxide, as seen by comparison of the ^{32}P-postlabeling profiles of adducts formed from DB[*a*,*l*]P and DB[*a*,*l*]P-11,12-dihydrodiol activated by microsomes (Figure 4).

FLN Spectroscopic Identification of Depurinating One-Electron Oxidation Adducts. Pilot fluorescence measurements at 77 K showed that the spectra of all four one-electron oxidation adduct standards were identical in shape and 5 nm red-shifted (0−0 band at 424 vs 419 nm), compared to the DB[*a*,*l*]P parent compound. Since line narrowing can only be expected upon excitation into the (weakly allowed) S_1 state, and the uncorrelated S_2 state lies rather close to the 0−0 transition (Nakhimovsky et al., 1989), only a small portion of the absorption spectrum (414−419 nm) is suitable for vibronically-excited FLN spectroscopy. Fortunately, this region contains a number of highly specific vibronic transitions, as shown in Figure 5, presenting the FLN spectra of the four adduct standards (solid upper curves). Although all of the one-electron oxidation adducts contain the same DB[*a*,*l*]P-type chromophore carrying the substituent at the same carbon atom (C-10), under FLN conditions the spectra are still remarkably different and very suitable for fingerprint identification. FLN spectra of the DB[*a*,*l*]P-10-N3Ade adduct are presented in Figure 5A. Comparison of the standard spectrum (upper curve) with that obtained for the corresponding adduct formed in the microsome reaction (dashed middle curve) illustrates the identification power of FLN spectroscopy. Matching spectra were obtained for six

Table 1: Quantitation of Biologically-Formed DB[*a*,*l*]P−DNA Adducts[a]

incubation system	total adducts (mol/mol of DNA−P) × 10^6	stable DNA adducts (mol/mol of DNA−P) × 10^6	depurinating DNA adducts (mol of adducts/mol of DNA−P) × 10^6					depurinating adducts (% of total)	ratio of depurinating to stable adducts
			DB[*a*,*l*]P-10-N3Ade	DB[*a*,*l*]P-10-N7Ade	DB[*a*,*l*]P-10-N7Gua	DB[*a*,*l*]P-10-C8Gua	*syn*-DB[*a*,*l*]PDE-14-N7Ade	*anti*-DB[*a*,*l*]PDE-14-N7Gua	
MC microsomes + DB[*a*,*l*]P									
native DNA	42	6.8 (16)[b]	12 (28)	5.9 (14)	1.0 (2)[c]	2.5 (6)	13 (31)	1.1 (3)	84	5.2
denatured DNA	13	5.8 (41)	<0.05	<0.05	<0.05	<0.05	7.1 (55)	0.6 (4)	59	1.3
MC microsomes + DB[*a*,*l*]P-11,12-dihydrodiol										
native DNA	139	112 (81)					25 (18)	1.8 (1)	19	0.24
denatured DNA	71	62 (87)					8.1 (12)	0.8 (1)	13	0.14
HRP	15	5.2 (35)	4.9 (33)[c]	4.0 (27)	0.7 (5)	<0.05			65	1.9

[a] Values are the average of determinations from at least two preparations. The amount of each adduct varied between 5% and 10% in the preparations, with larger variations with the minor adducts. [b] Number in parentheses is percentage of total adducts. [c] This value is probably overestimated because low-temperature fluorescence revealed the presence of an unidentified coeluting compound.

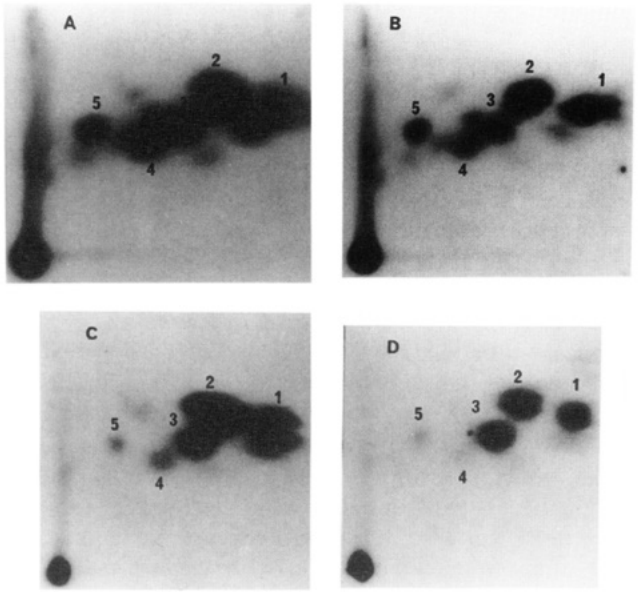

FIGURE 4: Autoradiogram of ^{32}P-postlabeled DNA-containing stable adducts formed by microsomal activation of (A) DB[*a*,*l*]P in the presence of native DNA, (B) DB[*a*,*l*]P in the presence of denatured DNA, (C) DB[*a*,*l*]P-11,12-dihydrodiol in the presence of native DNA, and (D) DB[*a*,*l*]P-11,12-dihydrodiol in the presence of denatured DNA. The film was exposed at room temperature for 90 min (A and B) or 7 min (C and D).

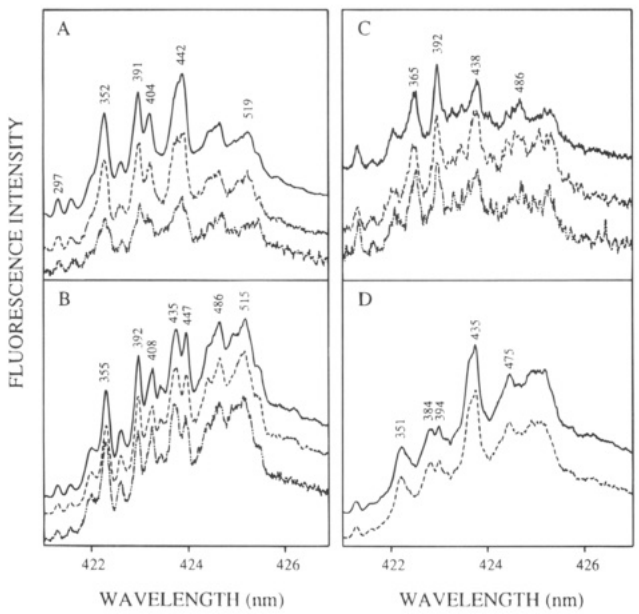

FIGURE 5: FLN spectroscopic identification of depurinating one-electron oxidation adducts. (A) DB[*a*,*l*]P-10-N3Ade, (B) DB[*a*,*l*]P-10-N7Ade, (C) DB[*a*,*l*]P-10-N7Gua, (D) DB[*a*,*l*]P-10-C8Gua. Solid upper curves, adduct standard solution; dashed middle curves, corresponding HPLC fraction of microsome-activated reaction; dashed−dotted lower curves (A−C only), corresponding HPLC fraction of HRP-activated reaction. Peaks are labeled with their excited state vibrational frequencies in wave numbers; intensities are not on scale; $T = 4.2$ K; $\lambda_{ex} = 416.08$ nm.

different excitation wavelengths (other spectra not shown). Weak spectra that matched those of the DB[*a*,*l*]P-10-N3Ade standard were also obtained from a depurinating adduct formed in the HRP-catalyzed reaction (dashed−dotted lower curve).

The HPLC fractions coeluting with the DB[*a*,*l*]P-10-N7Ade standard indeed contained that compound (Figure 5B) both in the rat liver microsome-activated reaction (dashed middle curve) and in the HRP-catalyzed reaction (dashed−dotted lower curve). The one-electron oxidation adduct with DB[*a*,*l*]P bound at C-10 to the N-7 of guanine was also positively identified in both *in vitro* systems (Figure 5C), although the noise levels in the spectra (dashed middle and dashed−dotted lower curves) indicate that the yields were much lower than for the adenine adducts (see also Table 1). DB[*a*,*l*]P-10-C8Gua (Figure 5D) was found only in the microsome-catalyzed reaction. The HRP reaction did yield a minor product with HPLC retention times identical with that of DB[*a*,*l*]P-10-C8Gua in both solvent systems, but its FLN spectrum did not match with any known adduct and the compound remains to be identified. This emphasizes the importance of applying a selective technique like FLNS for independent structure confirmation of HPLC fractions.

FLN Spectroscopic Identification of Depurinating Diol Epoxide Adducts. Pilot fluorescence measurements at 77 K (not shown) revealed important spectral differences between the two diol epoxide adduct standards. Although both adducts contain the same benzo[*e*]pyrene-type chromophore, the *syn*-DB[*a*,*l*]PDE-14-N7Ade adduct shows a spectrum that is 6 nm red-shifted compared to benzo[*e*]pyrene, whereas the spectrum of the *anti*-DB[*a*,*l*]PDE-14-N7Gua adduct is broader and 13−14 nm red-shifted. More detailed FLNS studies in different solvents and quantum mechanical calculations indicate that this effect is probably related to different conformational equilibria (unpublished results). The focus of this paper, however, is only on identification by means of FLN spectroscopy.

The FLN spectra obtained for *syn*-DB[*a*,*l*]PDE-14-N7Ade are shown in Figure 6A. The solid upper curve was obtained for the standard adduct. The matching dashed middle curve and dashed−dotted lower curve show that the same compound is produced in the microsome-activated reactions from DB[*a*,*l*]P and DB[*a*,*l*]P-11,12-dihydrodiol, respectively.

The FLN spectra of the *anti*-DB[*a*,*l*]PDE-14-N7Gua adduct are shown in Figure 6B,C. Synthesis of this adduct standard yielded a mixture of diastereoisomers with *cis* and *trans* opening of the epoxy ring. The two compounds have practically identical retention times on HPLC in both solvent systems, but they may be distinguished on the basis of their FLN spectra, as shown by the solid curves in Figure 6B,C. The vibrational frequencies in Figure 6B are very similar to (though not identical with) those obtained for *trans* opening of *anti*-DB[*a*,*l*]PDE in reaction with dA (unpublished results). On the other hand, the vibrational pattern of Figure 6C is similar to that of *cis* opening of *anti*-DB[*a*,*l*]PDE plus dA. The adducts in Figure 6B,C are thus thought to have *trans* and *cis* stereochemistry, respectively. Interestingly, the microsome-activated reaction with DB[*a*,*l*]P yielded primarily the *trans* diastereomer of *anti*-DB[*a*,*l*]PDE-14-N7Gua (Figure 6B, dashed curve), whereas the *cis* adduct was identified as a product of the reaction with microsome-activated DB[*a*,*l*]P-11,12-dihydrodiol (Figure 6C, dashed curve).

Quantitation of DNA Adducts. Quantitation of stable adducts was accomplished by the ^{32}P-postlabeling method, whereas quantitation of depurinating adducts was achieved by HPLC with a radiation flow monitor. With microsomal activation, about 15 times more stable adducts were formed from the dihydrodiol than from the parent DB[*a*,*l*]P (Table 1). Among the six depurinating adducts of DB[*a*,*l*]P, the three major ones were the adenine adducts (±)-*syn*-DB[*a*,*l*]-

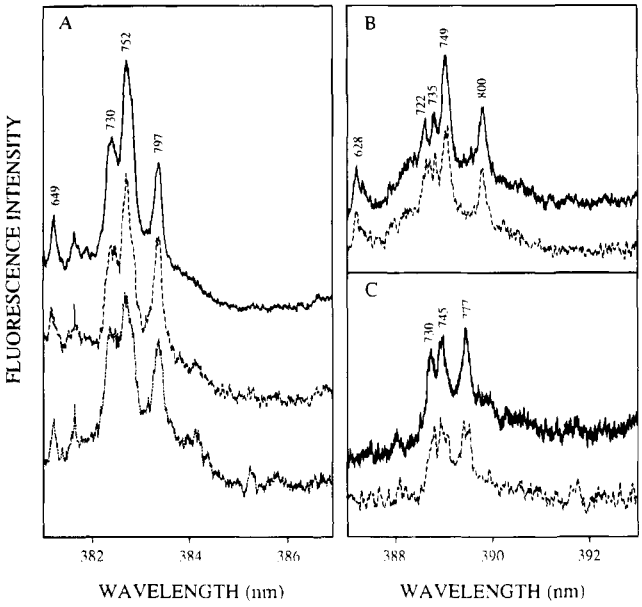

FIGURE 6: FLN spectroscopic identification of depurinating diol epoxide adducts. (A) *syn*-DB[*a*,*l*]PDE-14-N7Ade, λ_{ex} = 372.00 nm. Solid upper curve, adduct standard solution; dashed middle curve, corresponding HPLC fraction from reaction with DB[*a*,*l*]P; dashed−dotted lower curve, corresponding HPLC fraction from reaction with DB[*a*,*l*]P-11,12-dihydrodiol. (B) *anti*-DB[*a*,*l*]PDE-14-N7Gua, tentatively identified as *trans* isomer at C-13 and C-14, λ_{ex} = 378.00 nm. Solid curve, adduct standard solution; dashed curve, corresponding HPLC fraction from reaction with DB[*a*,*l*]P. (C) *anti*-DB[*a*,*l*]PDE-14-N7Gua, tentatively identified as *cis* isomer, λ_{ex} = 378.00 nm. Solid curve, adduct standard solution; dashed curve, corresponding HPLC fraction from reaction with DB[*a*,*l*]P-11,12-dihydrodiol. Peaks are labeled with their excited state vibrational frequencies in wave numbers; intensities are not on scale; T = 4.2 K. See, also, the text.

PDE-14-N7Ade (31%), formed by monooxygenation, and DB[*a*,*l*]P-10-N3Ade (28%) and DB[*a*,*l*]P-10-N7Ade (14%), formed by one-electron oxidation (Table 1). With DB[*a*,*l*]P-11,12-dihydrodiol, the predominant depurinating adduct was (±)-*syn*-DB[*a*,*l*]PDE-14-N7Ade. Although this adduct represented a much lower percentage of total adducts because the dihydrodiol formed so high an amount of stable adducts, the actual amount of (±)-*syn*-DB[*a*,*l*]PDE-14-N7Ade was about 2 times the amount formed from the parent compound under comparable conditions (Table 1).

Activation of DB[*a*,*l*]P by HRP yielded predominantly depurating adducts. Only three depurinating adducts were detected, but the major ones, DB[*a*,*l*]P-10-N3Ade and DB-[*a*,*l*]P-10-N7Ade, were also the major depurinating adducts in microsome-catalyzed one-electron oxidation.

DB[a,l]P Adducts Formed with Denatured DNA. As already observed for BP (Rogan et al., 1993) and DMBA (Devanesan et al., 1993), denatured DNA did not support formation of depurinating adducts by one-electron oxidation (Table 1). The adducts DB[*a*,*l*]P-10-N3Ade, DB[*a*,*l*]P-10-N7Ade, DB[*a*,*l*]P-10-N7Gua, and DB[*a*,*l*]P-10-C8Gua were not detected when DB[*a*,*l*]P was activated by microsomes. These results imply that double-stranded DNA is required for the reaction of the DB[*a*,*l*]P radical cation at the N-3 or N-7 of adenine and the N-7 or C-8 of guanine. In contrast, (±)-*syn*-DB[*a*,*l*]PDE-14-N7Ade and (±)-*anti*-DB[*a*,*l*]PDE-14-N7Gua were formed with single-stranded DNA, although in smaller amounts than with native DNA. When DB[*a*,*l*]P-11,12-dihydrodiol was activated by microsomes in the presence of single-stranded DNA, the two diol epoxide adducts were formed, but again in smaller amounts than with native DNA (Table 1).

DISCUSSION

Activation of DB[*a*,*l*]P by cytochrome P-450 in the presence of DNA yields predominantly depurinating adducts, formed by one-electron oxidation and the diol epoxide pathway. This finding is similar to those observed with BP (Devanesan et al., 1992; Rogan et al., 1993) and DMBA (Devanesan et al., 1993; RamaKrishna et al., 1992a). Although with BP and DMBA the major depurinating adducts are formed by one-electron oxidation, the major depurinating adducts of DB[*a*,*l*]P are obtained from both pathways (Table 1).

Activation of DB[*a*,*l*]P-11,12-dihydrodiol by cytochrome P-450 produces two depurinating adducts, of which (±)-*syn*-DB[*a*,*l*]PDE-14-N7Ade is the predominant one. In this case, most of the adducts are stable (81%) and only 19% are depurinating adducts (Table 1). These results are very similar to those observed with microsomal activation of BP and its corresponding 7,8-dihydrodiol, in which the ratio of depurinating to stable adducts is about 4 with the parent compound and about 0.2 with the dihydrodiol (Devanesan et al., 1992; Rogan et al., 1993). The ratio of depurinating to stable adducts is even more dramatic for BPDE reacted with DNA (0.02), in which 98% are stable adducts, and their level is about 25 times more than that of BP bound to DNA by microsomes and 3 times more than that of BP-7,8-dihydrodiol activated by microsomes (Devanesan et al., 1992).

The carcinogenicity of BP-7,8-dihydrodiol is similar to that of BP in mouse skin but much less than that of BP in rat mammary gland (Cavalieri et al., 1988; Levin et al., 1977; Slaga et al., 1976). In turn, the carcinogenicity of BPDE is much less than that of BP and BP-7,8-dihydrodiol (Levin et al., 1977; Slaga et al., 1977). Similar results have been observed with DB[*a*,*l*]P, in which the parent compound is more carcinogenic than its 11,12-dihydrodiol, which in turn is much more active than the *syn*- and *anti*-DB[*a*,*l*]P-diol epoxides (Cavalieri et al., 1991; Gill et al., 1994; Higginbotham et al., 1993). Thus, it seems from these initial results that turmorigenicity is not related to the level of stable adducts. Instead, depurinating adducts may contribute more to the tumorigenicity of these PAH than do stable adducts.

The profiles of the stable DB[*a*,*l*]P and DB[*a*,*l*]P-11,12-dihydrodiol adducts seen by ^{32}P-postlabeling (Figure 4) are qualitatively similar, indicating that cytochrome P-450 activation of DB[*a*,*l*]P produces stable adducts primarily formed from the diol epoxides.

With single-stranded DNA, activation of DB[*a*,*l*]P by cytochrome P-450 does not afford depurinating adducts formed by one-electron oxidation but produces smaller amounts of depurinating adducts by the diol epoxide pathway (Table 1). The stable adducts are qualitatively and quantitatively similar to those formed with double-stranded DNA. With DB[*a*,*l*]P-11,12-dihydrodiol, single-stranded DNA produces a smaller amount of stable and depurinating adducts compared to the corresponding profile with native DNA. The lack of depurinating adducts formed by one-electron oxidation of DB[*a*,*l*]P with single-stranded DNA indicates that the double-helical structure of DNA is required for formation of adducts by this mechanism. These results are analogous

to those obtained with BP and DMBA (Devanesan et al., 1993; Rogan et al., 1993).

The major depurinating adducts of DB[*a*,*l*]P formed by both mechanisms of activation are those with the PAH bound to the N-3 and N-7 of Ade (73%, Table 1). This is similar to that found with microsomal activation of DB[*a*,*l*]P-11,-12-dihydrodiol, in which (±)-*syn*-DB[*a*,*l*]PDE-14-N7Ade constitutes 95% of the depurinating adducts detected. Predominance of an N7Ade adduct was also observed with DMBA (Devanesan et al., 1993; RamaKrishna et al., 1992a). When these adducts are released from DNA, they leave behind an apurinic site, which if not repaired can be mutagenic (Loeb & Preston, 1986).

REFERENCES

Bodell, W. J., Devanesan, P. D., Rogan, E. G., & Cavalieri, E. L. (1989) *Chem. Res. Toxicol. 2*, 312−315.

Cavalieri, E., & Rogan, E. (1985) *Environ. Health Perspect. 64*, 69−84.

Cavalieri, E., & Rogan, E. (1992) *Pharmacol. Ther. 55*, 183−199.

Cavalieri, E., Rogan, E., Higginbotham, S., Cremonesi, P., & Salmasi, S. (1988) *J. Cancer Res. Clin. Oncol. 114*, 16−22.

Cavalieri, E. L., Rogan, E. G., Higginbotham, S., Cremonesi, P., & Salmasi, S. (1989) *J. Cancer Res. Clin. Oncol. 115*, 67−72.

Cavalieri, E. L., Rogan, E. G., Devanesan, P. D., Cremonesi, P., Cerny, R. L., Gross, M. L., & Bodell, W. J. (1990) *Biochemistry 29*, 4820−4827.

Cavalieri, E. L., Higginbotham, S., RamaKrishna, N. V. S., Devanesan, P. D., Todorovic, R., Rogan, E. G., & Salmasi, S. (1991) *Carcinogenesis 12*, 1939−1944.

Conney, A. H. (1982) *Cancer Res. 42*, 4875−4917.

Devanesan, P. D., Cremonesi, P., Nunnally, J. E., Rogan, E. G., & Cavalieri, E. L. (1990) *Chem. Res. Toxicol. 3*, 580−586.

Devanesan, P. D., RamaKrishna, N. V. S., Todorovic, R., Rogan, E. G., Cavalieri, E. L., Jeong, H., Jankowiak, R., & Small, G. J. (1992) *Chem. Res. Toxicol. 5*, 302−309.

Devanesan, P. D., RamaKrishna, N. V. S., Padmavathi, N. S., Higginbotham, S., Rogan, E. G., Cavalieri, E. L., Marsch, G. A., Jankowiak, R., & Small, G. J. (1993) *Chem. Res. Toxicol. 6*, 364−371.

Gill, H. S., Kole, P. L., Wiley, J. C., Li, K.-M., Higginbotham, S., Rogan, E. G., & Cavalieri, E. L. (1994) *Carcinogenesis 15*, 2455−2460.

Higginbotham, S., RamaKrishna, N. V. S., Johansson, S. L., Rogan, E. G., & Cavalieri, E. L. (1993) *Carcinogenesis 14*, 875−878.

IARC (1983) *IARC Monographs on the Evaluation of Carcinogenic Risk of Chemicals to Humans, Vol. 32, Polynuclear Aromatic Compounds, Part 1, Chemical, Environmental and Experimental Data*, pp 33−104, 327−347, IARC, Lyon.

Jankowiak, R., & Small, G. J. (1991) *Chem. Res. Toxicol. 4*, 256−269.

Jeffrey, A. M., Jennette, K. W., Blobstein, S. H., Weinstein, I. B., Beland, F. A., Harvey, R. G., Kasai, H., Miura, I., & Nakanishi, K. (1976) *J. Am. Chem. Soc. 98*, 5714−5715.

Koreeda, M., Moore, P. D., Wislocki, P. G., Levin, W., Conney, A. H., Yagi, H., & Jerina, D. M. (1978) *Science (Washington, D.C.) 199*, 778−781.

LaVoie, E. J., He, J.-M., Meegalla, R. L., & Weyand, E. H. (1993) *Cancer Lett. 70*, 7−14.

Levin, W., Wood, A. W., Wislocki, P. G., Kapitulnik, J., Yagi, H., Jerina, D. M., & Conney, A. H. (1977) *Cancer Res. 37*, 3356−3361.

Li, K.-M., RamaKrishna, N. V. S., Padmavathi, N. S., Rogan, E. G., & Cavalieri, E. L. (1994) *Polycyclic Aromat. Compd. 6*, 207−213.

Li, K.-M., RamaKrishna, N. V. S., Cavalieri, E. L., Rogan, E. G., Cerny, R. L., George, M., & Gross, M. L. (1995a) *Chem. Res. Toxicol.* (submitted for publication).

Li, K.-M., Rogan, E. G., & Cavalieri, E. L. (1995b) *Proc. Am. Assoc. Cancer Res. 36*, 137.

Loeb, L. A., & Preston, B. D. (1986) *Annu. Rev. Genet. 20*, 201−230.

Mumford, J. L., Harris, D. B., & Williams, K. (1987) *Environ. Sci. Technol. 21*, 308−311.

Mumford, J., Li, X., Hu, F., Lu, X., Chuang, J. (1995) *Proc. Am. Assoc. Cancer Res. 36*, 109.

Nakhimovsky, L. A., Lamotte, M., & Joussot-Dubien, J. (1989) *Handbook of Low Temperature Electronic Spectra of Polycyclic Aromatic Hydrocarbons*, pp 489−490, Elsevier, Amsterdam.

RamaKrishna, N. V. S., Devanesan, P. D., Rogan, E. G., Cavalieri, E. L., Jeong, H., Jankowiak, R., & Small, G. J. (1992a) *Chem. Res. Toxicol. 5*, 220−226.

RamaKrishna, N. V. S., Gao, F., Padmavathi, N. S., Cavalieri, E. L., Rogan, E. G., Cerny, R. L., & Gross, M. L. (1992b) *Chem. Rex. Toxicol. 5*, 293−302.

RamaKrishna, N. V. S., Padmavathi, N. S., Cavalieri, E. L., Rogan, E. G., Cerny, R. L., & Gross, M. L. (1993) *Chem. Res. Toxicol. 6*, 554−560.

Rogan, E. G., Katomski, P. A., Roth, R. W., & Cavalieri, E. L. (1979) *J. Biol. Chem. 254*, 7055−7059.

Rogan, E. G., Cavalieri, E. L., Tibbels, S. R., Cremonesi, P., Warner, C. D., Nagel, D. L., Tomer, K. B., Cerny, R. L., & Gross, M. L. (1988) *J. Am. Chem. Soc. 110*, 4023−4029.

Rogan, E. G., Devanesan, P. D., RamaKrishna, N. V. S., Higginbotham, S., Padmavathi, N. S., Chapman, K., Cavalieri, E. L., Jeong, H., Jankowiak, R., & Small, G. J. (1993) *Chem. Res. Toxicol. 6*, 356−363.

Sims, P., & Grover, P. L. (1981) in *Polycyclic Hydrocarbons and Cancer* (Gelboin, H. V., & Ts'o, P. O. P., Eds.) pp 117−181, Academic Press, New York.

Slaga, T. J., Viaje, A., Berry, D. L., Bracken, W., Buty, S. G., & Scribner, J. D. (1976) *Cancer Lett. 2*, 115−122.

Slaga, T. J., Bracken, W. M., Viaje, A., Levin, W., Yagi, H., & Jerina, D. M. (1977) *Cancer Res. 37*, 4130−4133.

Snook, M. E., Severson, R. F., Arrendale, R. F., Higman, H. C., & Chortyk, O. T. (1977) *Beitrag. Tabakforsch. 9*, 79−101.

BI942700K